

See discussions, stats, and author profiles for this publication at: <https://www.researchgate.net/publication/231231484>

Domain Matching Epitaxy of Mg-Containing Ag Contact on p-Type GaN

ARTICLE *in* CRYSTAL GROWTH & DESIGN · MAY 2011

Impact Factor: 4.89 · DOI: 10.1021/cg200323h

CITATIONS

5

READS

39

7 AUTHORS, INCLUDING:



Jun Ho Son

University of California, Berkeley

39 PUBLICATIONS 310 CITATIONS

SEE PROFILE



Hak Ki Yu

Ajou University

37 PUBLICATIONS 332 CITATIONS

SEE PROFILE



A Facile Method for Morphological Control of MgZnO Nanostructures on GaAs Substrates and Their Optical Properties

Ju Ho Lee¹, Dong Chan Kim², Sooyeon Hwang¹, Jeong Yong Lee¹, and Hyung Koun Cho^{3,*}

¹Department of Materials Science and Engineering, KAIST, Daejeon 305-701, Republic of Korea

²OLED Research Team 2, Samsung Mobile Display, San 24 Nonseo-dong, Giheung-gu, Yongin 446-711, Republic of Korea

³School of Advanced Materials Science and Engineering, Sungkyunkwan University, 300 Cheoncheon-dong, Jangan-gu, Suwon, Gyeonggi-do 440-746, Republic of Korea

This research reports on morphological changes depending on the growth temperature in MgZnO nanostructures grown on GaAs substrates by metalorganic chemical vapor deposition as well as the investigation of their optical properties. As the growth temperature increased, the morphology of the MgZnO nanostructure changed from one-dimensional nanowires (480 °C) to pseudo-two-dimensional nanowalls (500 °C) to pyramid-shaped structures (520 °C). Among these structures, the nanowalls exhibited the best optical properties due to the large active surface area and high crystalline quality.

Keywords: MgZnO, Microstructure, Nanowires, Nanowalls, TEM, GaAs.

1. INTRODUCTION

Recently, various types of low-dimensional ZnO nanostructures, such as nanowires,¹ nanawalls,² and nanorings,³ have been studied for the applications in optoelectronic devices, energy harvesting, and various sensors. Among several substrates, GaAs has a direct bandgap and a small band offset of 0.23 eV with ZnO.⁴ Also, the *p*-type formation of GaAs is easier than that of ZnO, which allows for the use of the GaAs substrates as a hole injection layer instead of *p*-type ZnO. Since GaAs has semiconducting conductivity, it is facile to fabricate *p*-*n* junction based nanodevice with vertical stacking. Despite the merits of GaAs as a substrate for the growth of ZnO nanostructures, there are only a few reports on the synthesis of ZnO nanostructures on GaAs substrates.^{5,6}

The purpose of this study is to present a facile method to control the morphology of high quality MgZnO nanostructures grown on GaAs substrates through the variation in growth temperature. Additionally, we investigate their microstructural and optical characteristics.

2. EXPERIMENTAL DETAILS

MgZnO nanostructures were grown on GaAs (001) substrates using low-pressure metalorganic chemical vapor

deposition (MOCVD). No metal catalysts were used to grow the MgZnO nanostructures, regardless of the morphology of the nanostructures. High purity diethylzinc (DEZn, 99.9995%) and oxygen gas (O₂, 99.9999%) were used as the Zn metalorganic source and oxidizer, respectively. Argon (Ar, 99.9999%) and bis-cyclopentadienyl-magnesium (Cp₂Mg, 99.9995%) were used as a carrier gas for the DEZn source and a precursor for Mg element, respectively. The growth of the MgZnO nanostructures was conducted at a reactor pressure of 1 Torr for 30 min. During the growth process, Zn and Mg flow rates were kept constant at 6.1 and 0.71 μmol/min, respectively.

To understand the effects of the growth temperature on the morphologies and microstructural characteristics of MgZnO nanostructures grown on GaAs substrates, the growth was performed at 480~520 °C with 20 °C steps. The morphologies and microstructural characteristics of the synthesized MgZnO nanostructures were investigated using high-resolution transmission electron microscopy (HRTEM, JEOL JEM-3010). To investigate optical properties of the MgZnO nanostructures, Raman measurements (HORIBA, LabRAM HR) were carried out using an Ar ion laser with wavelength of 514 nm. In addition, room-temperature photoluminescence (PL) measurements were performed using a 325 nm line from a He–Cd laser with low excitation intensity.

* Author to whom correspondence should be addressed.

3. RESULTS AND DISCUSSION

Figure 1 shows cross-sectional TEM image of sample grown at 480 °C. MgZnO nanowires with heights of $\sim 1.95 \mu\text{m}$ and widths of $\sim 11 \text{ nm}$ were vertically synthesized on GaAs substrates, as shown in Figure 1(a).

There is a transition layer which was composed of columns between bottoms of the nanowires and the substrate, and this transition mainly consisted of 32° side facets with respect to the $(0002)_{\text{MgZnO}}$ plane [Fig. 1(b)]. Based on the crystallographic angular relations in the wurtzite ZnO, the 32° side facets were identified as $\{10\bar{1}3\}_{\text{MgZnO}}$ planes with high surface energy. As the growth process continued, the $\{10\bar{1}3\}_{\text{MgZnO}}$ planes changed to $\{10\bar{1}0\}_{\text{MgZnO}}$ planes due to the lowered surface energy, and finally, 1D MgZnO nanowires were formed on the top of the transition layer.

Figure 2(a) shows cross-sectional TEM image of the sample grown at 500 °C, which indicated the synthesis of MgZnO nanowalls. It is noticeable that the top facets of the synthesized nanowalls have an angle of 22° with respect to the $(0002)_{\text{MgZnO}}$ plane. The 22° top facets of the nanowalls were frequently observed in previous studies on the synthesis of the ZnO nanowalls, regardless of the growth methods and conditions,^{6–8} but the formation mechanism is still in question. The major planes of the synthesized MgZnO nanowalls are $\{11\bar{2}0\}_{\text{MgZnO}}$ planes and the resulting nanowalls show high crystalline quality without defects, such as stacking faults, as shown in Figure 2(b). The detailed growth mechanism and microstructural characteristics of the MgZnO nanowalls were described in Ref. [6].

The sample grown at 520 °C showed the 3D-like pyramid-shaped MgZnO structures, as shown in Figure 3(a). The dominant side facets observed in the pyramid-shaped structures were inclined with an angle of approximately 71° with respect to the $(0002)_{\text{MgZnO}}$ plane. However, there are no planes which have an angle of 71° with respect to the $(0002)_{\text{MgZnO}}$ plane in the wurtzite ZnO. Thus, for more detailed analysis, we performed

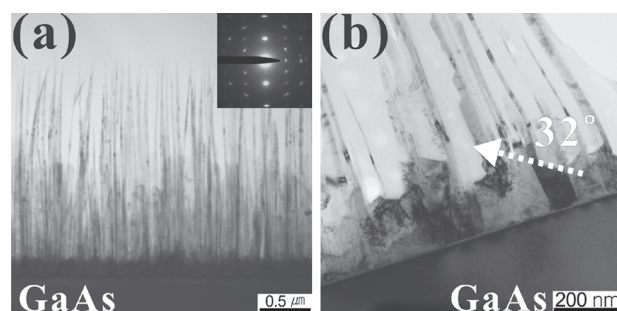


Fig. 1. (a) Cross-sectional TEM image of 480 °C grown sample. (b) Enlarged cross-sectional TEM image taken from near the interface between the MgZnO nanowires and GaAs substrate.

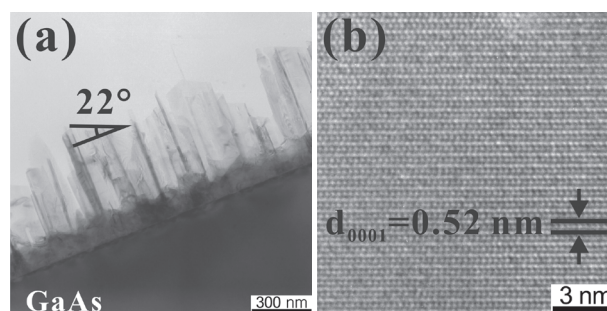


Fig. 2. (a) Cross-sectional TEM image of 500 °C grown sample. (b) Cross-sectional HRTEM image along the $[11\bar{2}0]_{\text{MgZnO}}$ zone axis of the nanowall.

HRTEM observation, as shown in Figures 3(b) and (c). It revealed that the inclined side facets of the pyramid-shaped structures consisted of high index planes with many dangling bonds, such as the $\{11\bar{2}2\}_{\text{MgZnO}}$ and $\{11\bar{2}4\}_{\text{MgZnO}}$ planes, except the $\{10\bar{1}0\}_{\text{MgZnO}}$ planes. The formation of a nanostructure with high index planes is energetically not favorable. However, due to the low melting temperature (419.53°C) of the Zn element, some of the Zn atoms deposited on the surface of nanostructure were can be desorbed from low index planes, and this may result in the formation of high index planes with high surface energy. In addition, the $\{10\bar{1}0\}_{\text{MgZnO}}$ planes with low surface energy were also formed and lowered the total surface energy of the pyramid-shaped MgZnO structures.⁹ Consequently, we found that the variation in the growth temperature induced

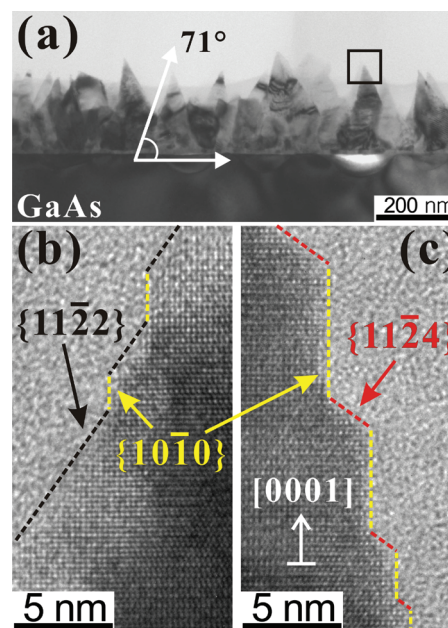


Fig. 3. (a) Cross-sectional TEM image of 520 °C grown sample. Enlarged HRTEM image of tip of pyramid-shaped structure from rectangular region marked by solid line in (a); (b) left and (c) right side facets of pyramid-shaped MgZnO structure.

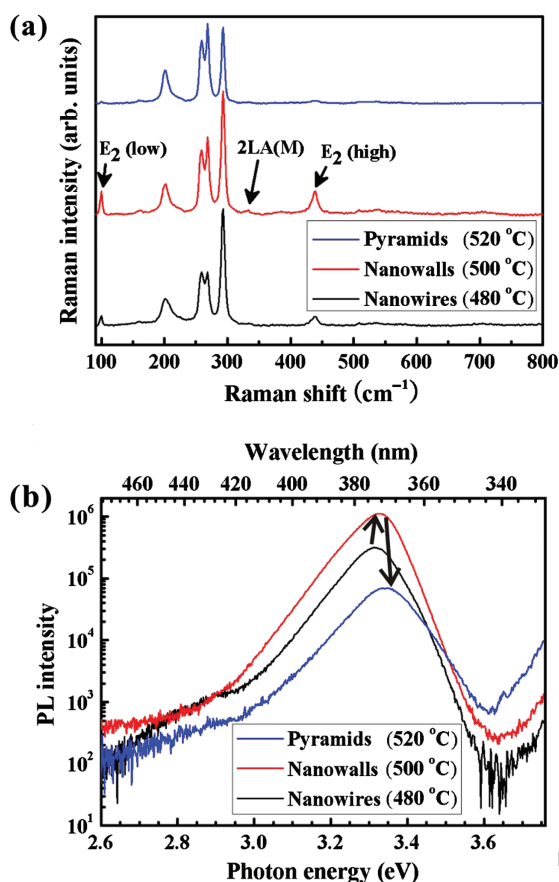


Fig. 4. (a) Raman and (b) room-temperature PL spectra of MgZnO nanostructures with various morphologies. Only the Raman peaks from the MgZnO nanostructures were indexed.

the morphological change from nanowires to nanowalls and pyramid-shaped nanostructures.

Figure 4(a) shows the Raman spectra for the MgZnO nanostructures with various morphologies. Regardless of morphological change, all peaks appeared at the same positions and only showed different intensities, as shown in Figure 4(a). This indicates that these samples contained the same amount of Mg due to the solubility limit (~ 4 at%), despite the different growth temperature.

The peaks at 100.4, 332.8, and 438.8 cm^{-1} corresponding to E_2 (low), 2LA (M), and E_2 (high), respectively. No LO-phonon peaks are observed from the MgZnO nanostructures, because the incident laser is perpendicular to the c -axis of the nanostructures.¹⁰ This is in good agreement with the TEM data showing the c -axis preferred orientation. Based on the intensity of the Raman spectra, the MgZnO layers with nanowall arrays show the best optical properties among the synthesized nanostructures. Figure 4(b) is the room-temperature PL spectra of the MgZnO nanostructures. As the morphology of the nanostructures changed from nanowires to nanowalls and pyramid-shaped structures, the PL peak continuously shifted to higher energy (i.e., blue shift). Because all the

resulting MgZnO nanostructures contain the same amount of Mg and the pyramid-shaped structure with larger width shows the highest photon energy, it was concluded that the blue shift was not due to the quantum confinement effect by the reduced size and different Mg contents. In addition, all the nanostructures have high crystalline quality because there are no visual defects, such as dislocations and stacking faults. The main reason for this may be related to the strain status induced by the different growth temperature. As the growth temperature increased, the thermal stress at the MgZnO/GaAs interface was increased. As a result, the residual strain in the MgZnO layers contributed to the peak shift to a higher energy.¹¹

The MgZnO nanowalls exhibited the highest PL intensity because of existence of large active surface area with high crystalline quality [Figs. 2(b and c)]. Therefore, among the three different morphologies of the MgZnO nanostructures controlled by growth temperature, it is expected that the nanowalls are the most suitable for sensor and solar cell applications. In addition, fabricating devices using the nanowalls is relatively simple due to the morphological characteristics.

4. CONCLUSION

We reported a facile method to control morphology of MgZnO nanostructures grown on GaAs substrates and investigated the microstructural change in the side facets of the nanostructures. As the growth temperature increased, the morphology of the MgZnO nanostructures changed from nanowires to nanowalls, and finally formed pyramid-shaped structures. Raman and PL measurements revealed that, among various nanostructures, the nanowalls exhibited the best optical properties. The morphologies of the MgZnO nanostructures on the GaAs substrates were easily controlled only by the growth temperatures in the MOCVD system.

Acknowledgment: This research was supported by the NRF of Korea funded by the MEST (Grant No. NRF-2008-314-D00153, NRF-2010-0002231 and NRF-2009-0078876).

References and Notes

1. L. Vayssieres, *Adv. Mater.* 15, 464 (2003).
2. D. C. Kim, J. H. Lee, S. K. Mohanta, H. K. Cho, and J. Y. Lee, *Nanotechnology* 21, 425503 (2010).
3. X. Y. Kong, Y. Ding, R. Yang, and Z. L. Wang, *Science* 303, 1348 (2004).
4. G. Du, U. Cui, X. Xiaochuan, X. Li, H. Zhu, B. Zhang, Y. Zhang, and Y. Ma, *Appl. Phys. Lett.* 90, 243504 (2007).
5. W. Lee, M.-C. Jeong, and J.-M. Myoung, *Nanotechnology* 15, 254 (2004).
6. J. H. Lee, D. C. Kim, J. Y. Lee, and H. K. Cho, *Cryst. Growth Des.* 10, 5205 (2010).

7. J. Shi, S. Grutzik, and X. Wang, *ACS Nano* 3, 1594 (2009).
8. X. Wang, Y. Ding, Z. Li, J. Song, and Z. L. Wang, *J. Phys. Chem. C* 113, 1791 (2009).
9. N. Fujimura, T. Nishihara, S. Goto, J. Xu, and T. Ito, *J. Cryst. Growth* 130, 269 (1993).
10. K. A. Alim, V. A. Fonoberov, M. Shamsa, and A. A. Balandin, *J. Appl. Phys.* 97, 124313 (2005).
11. J. K. Lee, C. R. Tewell, R. K. Schulze, M. Nastasi, D. W. Hamby, D. A. Lucca, H. S. Jung, and K. S. Hong, *Appl. Phys. Lett.* 86, 183111 (2005).

Received: 30 November 2010. Accepted: 31 January 2011.

Delivered by Ingenta to:
Korea Advanced Institute of Science & Technology (KAIST)
IP : 143.248.115.58
Thu, 15 Sep 2011 04:49:37